UNIVERSITY of York

This is a repository copy of *Opacity effects on laser-produced plasma radiation sources*.

White Rose Research Online URL for this paper:
http://eprints.whiterose.ac.uk/150167/

Version: Accepted Version

Article:

Tallents, Gregory John orcid.org/0000-0002-1409-105X (2019) Opacity effects on laser-produced plasma radiation sources. Journal of Applied Physics. 083302. ISSN 0021-8979

https://doi.org/10.1063/1.5111720

Reuse
Items deposited in White Rose Research Online are protected by copyright, with all rights reserved unless indicated otherwise. They may be downloaded and/or printed for private study, or other acts as permitted by national copyright laws. The publisher or other rights holders may allow further reproduction and re-use of the full text version. This is indicated by the licence information on the White Rose Research Online record for the item.

Takedown
If you consider content in White Rose Research Online to be in breach of UK law, please notify us by emailing eprints@whiterose.ac.uk including the URL of the record and the reason for the withdrawal request.

White Rose university consortium
Universities of Leeds, Sheffield & York

eprints@whiterose.ac.uk
https://eprints.whiterose.ac.uk/

Opacity effects on laser-produced plasma radiation sources

G. J. Tallents[1, a)]
York Plasma Institute, Department of Physics, University of York, York YO10 5DD, U.K.

(Dated: 29 July 2019)

The escape of spectral line radiation from laser-produced plasma radiation sources with moderate opacity is examined using a simple model of emission with a planar geometry, constant source function and an empirically determined optical depth. The model is applied to a determination of the radiation produced by laser irradiation of tin targets used as the source of radiation in extreme ultraviolet (EUV) lithography. Variations in emission relative to optically thin plasmas in agreement with previous experimental measurements of both the angular variation of the emission of EUV light at 13.5 nm and the effect of plasma opacity in reducing EUV emission at laser intensities above 10^{11} Wcm^{-2} are found. The model is extended to predict optimum conditions for future lithography radiation sources at ≈ 6.7 nm.

I. INTRODUCTION

Short wavelength sources in the extreme ultraviolet (EUV) and X-ray have been developed for many applications. Electrons accelerated in synchrotrons provide a range of controllable photon energies for experiments. More recently free electron lasers have been commissioned. With free electron lasers, stimulated emission in the EUV to X-ray range produces intense, collimated radiation within a narrow spectral bandwidth[1]. Laser-produced plasmas offer several routes to the production of EUV and X-ray radiation using smaller scale facilities. Electrons can be accelerated in laser-plasmas and then used for EUV and X-ray production[2]. Alternatively, the laser-produced plasma itself can be utilized as a source of EUV and X-ray radiation.

A major industrial application of EUV radiation is in the extreme ultraviolet lithography of semiconductors where the feature sizes that can be produced are proportional to the wavelength of the radiation source. The peak reflectivity of multi-layer mirrors consisting of alternating layers of Mo/Si at wavelength 13.5 nm has been found to be up to approximately 70% in a 4.5% bandwidth. The shorter wavelength 13.5 nm has, consequently, been selected to replace ArF excimer laser lithography at 193 nm in the manufacture of semiconductors[3]. The 13.5 nm radiation is produced with efficiencies up to a few percent in plasmas created by irradiating targets containing tin with focused laser light of intensity $\approx 10^{11}$ Wcm^{-2}. Tin at temperatures from 20 - 60 eV exhibits ionization from Sn^{7+} to Sn^{13+} with strong emission near 13.5 nm arising from unresolved transition arrays of form $4p^6 4d^n - 4p^5 4d^{n+1}$ and $4d^n - 4d^{n-1}4f$ (see O'Sullivan et al[4]). To minimize target debris, liquid tin dropped into the laser focal position is used in extreme ultraviolet lithography with large Mo/Si mirrors collecting the EUV emission from a large solid angle and focusing it to an intermediate focus. The radiation is typically collected over almost a hemisphere of 2π solid angle in the direction back towards the laser. After the intermediate focus, the EUV light is relayed via multilayer mirrors to expose photo-resist over a large area on a silicon wafer.

We examine the intensity of spectral lines from a planar plasma geometry and show the effects of moderate levels of opacity by integrating the radiation escaping the source in angle and frequency. Our results are compared to the equivalent optically thin emission giving values known as escape factors[5,6,7,8,9]. We compare our calculated reductions in the intensity emitted to some previously observed intensity variations in angle and in the laser intensity creating laser-produced plasmas. We concentrate on the effects of opacity arising in EUV sources from tin targets due to the industrial importance in EUV lithography.

II. THEORY

Opacity effects on plasma emission can be simplified by replacing spatial distances with optical depth and by replacing the emission coefficient for an element of plasma by the source function[5]. Optical depth is determined from the integration of the absorption coefficient over distance, while the source function is determined from the ratio of the emission coefficient to the absorption coefficient. In this formulation, spatial integration is equivalent to optical depth integration, so that an element of plasma exhibiting a planar symmetry with a spatially uniform source function S_0 emits radiation of intensity $I(\theta)$ varying with angle θ to the normal of the plane of symmetry such that

$$I(\theta) = \int_0^\tau S_0 e^{-\tau'/u} \frac{d\tau'}{u}$$

$$= S_0 \left(1 - e^{-\tau/u}\right) \quad (1)$$

where τ is the optical depth normal to the planes of symmetry and $u = \cos\theta$. For a planar source occupying a finite area, the finite area subtends a solid angle proportional to $1/u$ and so the intensity detected varies as $I(\theta)u$. We mainly determine intensities relative to optically thin intensities so do not need to consider this foreshortening as it effects both optically thick and optically thin intensities. However, for section III in a comparison to experimental intensities from a planar laser-produced plasma focal area, we present some values of $I(\theta)u$.

The source function is given by

$$S_0 = \frac{\varepsilon}{K} \quad (2)$$

a) Electronic mail: greg.tallents@york.ac.uk

where ε is the emission coefficient and K is the absorption coefficient. The optical depth τ is evaluated by integrating the absorption coefficient K over distances along the normal to the planes of symmetry. Many plasma radiation sources have an approximately constant source function as the emission coefficient and absorption coefficient have similar density variations which cancel in determining a value for the source function. Similarly, spectral line emission usually exhibits a source function S_0 which is approximately constant with frequency ω as the emission and absorption coefficients have similar or identical line profiles.

The optically thin intensity emitted by a plasma if there is no absorption is evaluated by integrating the emission coefficient ε along a line-of-sight. For an infinite planar geometry, the optically thin emission is $\int \varepsilon \, d(z/u)$ along a line-of-sight at angle θ to the normal to the planes of symmetry with $u = \cos\theta$. Assuming a constant source function $S_0 = \varepsilon/K$, this expression for the optically thin emission can be manipulated into the source function form by noting that

$$\int \varepsilon \, d(z/u) = \int (\varepsilon/K) K d(z/u) = (\varepsilon/K) \int K dz/u = S_0 \tau/u$$

where the optical depth τ is evaluated by integrating the absorption coefficient K in the z-direction (normal to the planes of symmetry). The expression $S_0\tau/u$ is the asymptotic intensity given by equation 1 for vanishingly small optical depths τ, but represents the optically thin emission for all optical depths. We calculate intensities in this paper relative to such optically thin values of emission: such relative intensities are often referred to as escape factors[5,6,7,8,9].

For an isotropic source function where we consider emission into a hemisphere solid angle, equation 1 can be integrated over angles θ between zero and $\pi/2$. The integration over vanishingly small optical depth τ becomes $S_0 2\pi\tau/u$, so we evaluate the ratio $< T(\theta) >$ of the angle integration at large τ to the small optical depth limit. We have

$$< T(\theta) >= \frac{1}{S_0 2\pi\tau} \int_{\theta=0}^{\pi/2} I(\theta) 2\pi \sin\theta \cos\theta \, d\theta$$

$$= \frac{1}{\tau} \int_{u=0}^{1} \left(1 - e^{\tau/u}\right) u \, du. \quad (3)$$

Values of $< T(\theta) >$ are shown in figure 1. Interestingly, a curve of the form of equation 1 fits the values of $< T(\theta) >$ if we replace τ by an angle averaged optical depth $< \tau >$. We find that the expression

$$< T(\theta) >_a = \frac{1}{< \tau >} \left(1 - e^{<\tau>}\right) \quad (4)$$

is a fit to $< T(\theta) >$ given by equation 3 if we set $< \tau >= 2\tau$ (see figure 1). This is equivalent to evaluating equation 1 with $u = 1/2$ corresponding to the evaluation when $\theta = 60$ degrees. We see that rays at an angle of 60 degrees to the normal to the planes of symmetry represent an 'average' ray that can be used in the evaluation of the fraction $< T(\theta) >$ of radiation escaping.

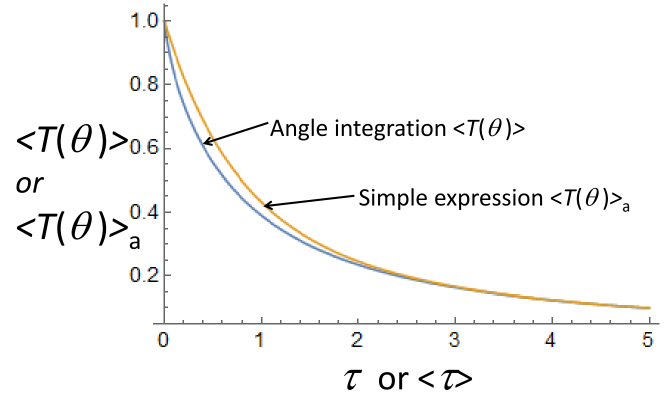

FIG. 1. The angle integrated intensity $< I(\theta) >$ as a function of optical depth τ along the normal to the planes of symmetry. A simple expression for $< I(\theta) >_a$ following equation 4 with $< \tau >= 2\tau$ is also shown.

The parameter $< T(\theta) >$ is an example of an escape factor. In agreement with our present results, Phillips et al[9] have previously recommended that an optical depth with value twice the optical depth normal to a plasma surface is used in escape factor evaluations in zero-dimensional radiation codes.

For radiation emission arising from spectral lines, the optical depth τ varies with frequency such that

$$\tau = \tau_0 \frac{f(\omega)}{f(0)} \quad (5)$$

where $f(\omega)$ is the value of the line profile function at frequency ω from line center and τ_0 is the optical depth normal to the planes of symmetry at line center where $\omega = 0$. We can modify equation 1 to obtain an expression for the intensity $I_T(\theta)$ of a spectral line integrated over frequency:

$$I_T(\theta) = S_0 \int_{\omega=-\infty}^{\infty} \left(1 - \exp\left(-\frac{\tau_0 f(\omega)}{f(0)u}\right)\right) d\omega. \quad (6)$$

The integrated intensities given by equation 6 depend on the line profile. We consider Gaussian and Lorentzian line profiles represented respectively by

$$f_g(\omega) = \frac{1}{\sqrt{\pi}} \exp(-\omega^2), \quad (7)$$

$$f_l(\omega) = \frac{1}{\pi} \frac{1}{1+\omega^2}. \quad (8)$$

The integration of these line profiles over all frequencies gives a value of one. At vanishingly small values of optical depth τ_0, the exponential in equation 6 can be expanded accurately to two terms to give optically thin intensities for respectively Gaussian and Lorentzian profiles

$$I_g(\omega) = S_0 \sqrt{\pi} \tau_0/u, \quad (9)$$

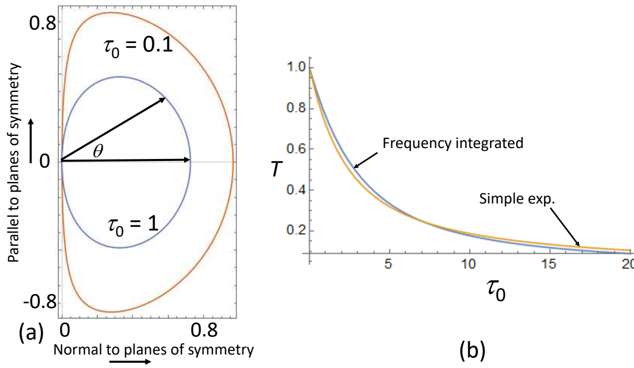

FIG. 2. (a) A polar plot showing the frequency integrated intensity of a spectral line with a Gaussian line profile as a function of angle θ to the normal to the planes of symmetry for optical depths τ_0 of 0.1 and 1 (as labeled). The intensities are divided by the optically thin intensity value $2\pi S_0\sqrt{\pi}\tau_0/u$. (b) The variation of the frequency integrated intensity for a Gaussian line profile along the normal to the planes of symmetry as a function of optical depth τ_0 (as labelled). The intensities are divided by the optically thin intensity value $S_0\sqrt{\pi}\tau_0$. Also shown is a simple expression of form $T = (1-\exp(-\tau_0/\sqrt{\pi}))/(\tau_0/\sqrt{\pi})$ that fits the frequency integrated intensity.

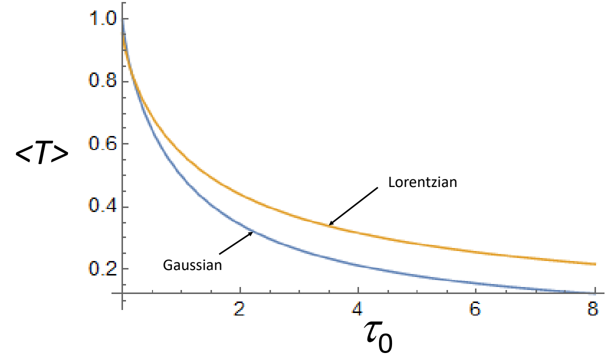

FIG. 3. The frequency and angle integrated intensity of a spectral line as a function of optical depth through a uniform slab relative to the optically thin intensity of the spectral line. Results are shown for Gaussian and Lorentzian line profiles (as labeled).

$$I_l(\omega) = S_0\pi\tau_0/u. \tag{10}$$

At non-vanishing optical depths, equation 6 needs to be numerically integrated (for example, see figure 2). Figure 2(a) shows that the angular variation at larger optical depth becomes closer to being Lambertian with a $\cos\theta$ variation of intensity. The variation of the frequency integrated intensity assuming a Gaussian line profile as a function of the peak value of the optical depth τ_0 at line centre (along the direction perpendicular to the planes of symmetry) is shown in Figure 2(b). The vertical axis (labeled T where $T = I_T(0)/(S_0\sqrt{\pi}\tau_0)$) is calculated using equation 6 and is plotted relative to the value given by equation 9: hence $T = 1$ at $\tau_0 = 0$. Figure 2(b) also presents a curve of the form of equation 1 which is similar to the numerically calculated variation. The simple expression that fits the numerical variation has the form

$$T_a = \frac{1-\exp(-\tau_0/\sqrt{\pi})}{\tau_0/\sqrt{\pi}}. \tag{11}$$

The fit of equation 11 to the numerically evaluated values of T in figure 2(b) shows that a frequency averaged optical depth τ_{av} is related to the optical depth τ_0 at line centre by $\tau_{av} = \tau_0/\pi^{1/2}$ for Gaussian line profiles. Similar calculations for Lorentzian profiles show that $\tau_{av} \approx \tau_0/\pi$. The proportionalities here are equal to the normalization constants required so that integration in frequency over the line profile is one: see equations 7 and 8.

The evaluated intensities can be further integrated over all angles. We are interested in the forward intensity into a half-sphere with rotational symmetry around the direction of the normal to the planes of symmetry and integrate the intensity relative to the optically thin intensity. Integration proceeds from angle θ parallel to the normal to the symmetry planes up to $\theta = \pi/2$ radians (parallel to the planes of symmetry). As obtained for equation 3, the integration is more readily solved using $u = \cos\theta$. Using equation 6 we can write:

$$< \frac{I_T(\theta)}{2\pi S_0} >= \int_{u=0}^{1}\int_{\omega=-\infty}^{\infty}\left(1-\exp\left(-\frac{\tau_0 f(\omega)}{f(0)u}\right)\right) u\, d\omega\, du. \tag{12}$$

As the angle integration is represented by an integration $u = 0$ to $u = 1$, the angle integrated intensities for vanishingly small values of optical depth τ_0 are similar to intensities given by equations 9 and 10 for respectively Gaussian and Lorentzian profiles with a simple 2π multiplier. The ratio $< T >$ of the angularly integrated intensities to the angularly integrated optically thin intensities is given by expressions of form for respectively Gaussian and Lorentzian profiles:

$$< T >=< \frac{I_T(\theta >}{2\pi S_0} > \frac{1}{\sqrt{\pi}\tau_0}, \tag{13}$$

$$< T >=< \frac{I_T(\theta}{2\pi S_0} > \frac{1}{\pi\tau_0} \tag{14}$$

where $< I_T(\theta)/2\pi S_0 >$ is evaluated using equation 12. We obtain values of $< T >$ varying only with optical depth τ_0 (see figure 3). The Gaussian curve shown in figure 3 can be fitted to within $\approx 10\%$ for optical depths τ_0 in the range zero to eight by an expression of the form of equations 4 and 11. The approximate fit to $< T >$ for the Gaussian curve shown in figure 3 is given by

$$< T >_a = \frac{1-\exp(-2\tau_0/\sqrt{\pi})}{2\tau_0/\sqrt{\pi}}. \tag{15}$$

Here, the factor 2 multiplying the optical depth τ_0 is associated with angle averaging, while the factor $1/\sqrt{\pi}$ is associated with the integration over frequency.

The escape factor values evaluated in this section apply for a planar geometry. Laser-produced plasmas created by irradiating solid planar targets or by irradiating expanding spherical droplets (as in EUV lithography) are a good approximation

to a finite area planar geometry as the focal width (typically $> 30\mu$m) significantly exceeds the ablation depth of emission and absorption. Ablation depths can be estimated (see equation 16) from the rate of ablation $\dot{m} \approx 3 \times 10^4$ gcm^{-2}s^{-1} (see Ng et al[10]) and laser pulse duration $t_L \approx 10^{-9} - 10^{-8}$ s as typically $\approx 0.1 - 3\mu$m.

III. COMPARISON WITH PUBLISHED EXPERIMENTAL RESULTS

The angular variation of extreme ultra-violet emission in a 2% bandwidth at 13.5 nm from a laser-produced tin plasma has been measured by Ando et al[11]. For the experiment, a laser of pulse duration 1 - 2 ns and wavelength 1.064 μm was focused to a diameter of $\approx 500\mu$m with intensity $10^{10} - 10^{12}$ Wcm^{-2} onto solid planar tin targets. The radiation detected from the planar layer of tin plasma extends only over the 500μm focal area and so the detected intensity varies with angle θ as $I_T(\theta)u$ because the subtended solid angle of the focal area at a detector reduces by $1/u = 1/\cos\theta$. We find that the evaluation of $I_T(\theta)u$ using equation 6 with optical depth $\tau_0 \approx 1$ is an approximate fit to the angular emission measured by Ando et al (see figure 4).

The emission at 13.5 nm arises from many spectral lines of tin. We assume a single spectral line in our analysis for equation 6, but provided the line profiles for each line do not overlap significantly and have the same profile shape (here, Gaussian or Lorentzian), equation 6 is applicable where there are many lines contributing to the emission. The angular variation of emission for the Ando et al experiment has also been analysed by Giavannini and Abharai[12]. The assumption of an infinite planar geometry for equation 6 breaks down at angle $\theta = 90$ degrees, so the experimental data point in figure 4 does not fit the $\tau_0 = 1$ calculated variation. Nevertheless, our analysis shows that a relatively simple evaluation assuming constant source function and a planar plasma geometry determines the angular variation of emission for angles $\theta < 90$ degrees.

Ando et al[11] used a value of $\sigma = 0.96 \times 10^5$ cm^{2}g^{-1} for the mass absorption coefficient of tin at 13.5 nm measured by Fujioka et a[13] to deduce a line profile averaged optical depth τ_{av} for a tin laser produced plasma at 13.5 nm. The calculation uses an estimate for the scaling of the depth d_A of ablation of a target of mass density ρ by a laser pulse of duration t_L given by

$$d_A = \frac{\dot{m}\, t_L}{\rho}, \tag{16}$$

where $\dot{m}$ is the mass ablation rate per unit area. Mass ablation rates vary with laser intensity I_l and laser wavelength λ_L, but are only weakly dependent on the target material[10,14]. Using the mass absorption coefficient σ and target density ρ, we have that the average optical depth is given by $\tau_{av} = \sigma\,\rho\, d_A$.

Using scalings for mass ablation rates $\dot{m}$ determined by Ng et al[10] at laser intensities greater than 10^{13} Wcm^{-2}, Ando et al[11] determined a scaling for the average optical depth at 13.5 nm for a tin laser-produced plasma. The mass ablation

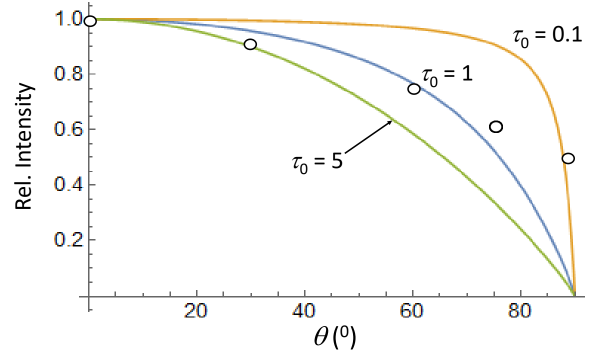

FIG. 4. The relative angular variation to the target normal of the emission for a spectral line with a Gaussian line profile with different optical depths τ_0 of an emission layer (as labelled). The angular variation of intensities at 13.5 nm measured by Ando et al[11] from a laser-plasma created from a plane tin target are shown as experimental data points.

rate scaling for tin with wavelength at laser intensities below 10^{13} Wcm^{-2}, however, has been shown[14] to vary as $\propto \lambda_L^{-4/9}$ rather than $\propto \lambda_L^{-4/3}$ (as considered by Ando et al[11]). The slower scaling of the ablation depth with wavelength λ_L occurs when absorption of the laser light is dominated by inverse bremsstrahlung absorption. Following the Ando et al[11] expression for the average optical depth at 13.5 nm for a tin laser-produced plasma, we obtain a similar variation of the average optical depth τ_{av} with laser intensity I_L and laser pulse duration t_L, but with a modified laser wavelength λ_L variation such that

$$\tau_{av} = 0.27 \left(\frac{I_L[\mathrm{Wcm^{-2}}]}{10^{11}}\right)^{5/9} \left(\frac{\lambda_L[\mu\mathrm{m}]}{1.064}\right)^{-4/9} t_L[\mathrm{ns}]. \tag{17}$$

Figure 2(b) indicates that the frequency averaged optical depth τ_{av} for a Gaussian line profile is related to the optical depth at line centre τ_0 by $\tau_{av} = \tau_0/\sqrt{\pi}$. A similar plot (not shown) for a Lorentzian line profile indicates that $\tau_{av} \approx \tau_0/\pi$. Keeping the focal spot diameter constant, experiments measuring the conversion efficiency of laser light energy to the energy emitted in the 13.5 nm spectral region using 1.064 μm radiation with pulse durations of several nanoseconds show a maximum conversion efficiency at laser intensities $I_L \approx 10^{11}$ Wcm^{-2} and a decrease at higher laser intensities. Consider an example for laser pulse duration $t_L = 2.2$ ns (see e.g. Ando et al[11], Fujioka et al[13]). The peak optical depth τ_0 varies with laser intensity I_L as

$$\tau_0 = C_{lp} \left(\frac{I_L[\mathrm{Wcm^{-2}}]}{10^{11}}\right)^{5/9} \tag{18}$$

where $C_{lp} = 1$ for a Gaussian line profile and $C_{lp} = \sqrt{\pi}$ for a Lorentzian line profile. Converting laser intensity I_L to optical depth τ_0 using equation 18 we can use the variation of $< T >$ shown in figure 3 to estimate the relative EUV emission as a function of laser intensity for an experiment where the focal spot diameter is constant (see figure 5). It is clear from figure 5

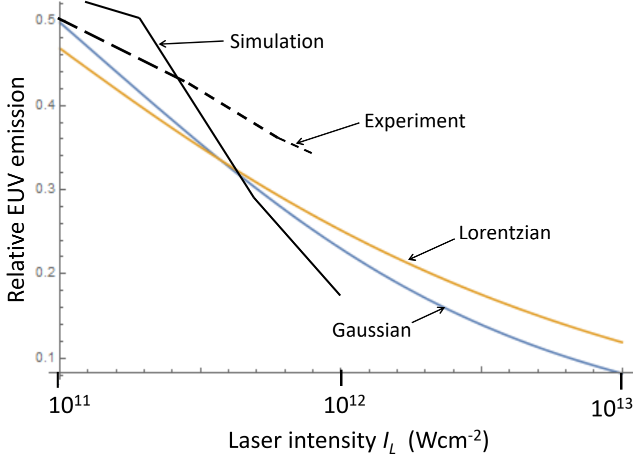

FIG. 5. The relative intensity of emission produced by optical depth changes associated with laser intensity variations in a laser-produced plasma. The appropriate relationship between optical depth τ_0 at line centre and laser intensity is given by equation 18 for Gaussian and Lorentzian profiles (as labeled). The vertical axis is the value of $< T >$ as shown in figure 3. Superimposed are simulation and experimentally measured relative EUV emission as shown in their figure 6 by Fujioka et al[13] (as labelled). The experimental and simulation values peak at $\approx$ 1.8% efficiency at laser intensity 10^{11} Wcm^{-2} and are scaled to our relative EUV emission values.

that the emitted EUV intensity can drop for $I_L > 10^{11}$ Wcm^{-2} solely due to the effect of increasing optical depth in the laser-produced plasma. Decreases in conversion efficiency of EUV emission at intensities above 10^{11} Wcm^{-2} have been observed in several experimental studies[11,13]. We have superimposed on figure 5 relative EUV emission at 13.5 nm as simulated and measured by Fujioka et al[13].

At laser intensities I_L on target less that 10^{11} Wcm^{-2} for the conditions of the Fujioka et al[13] experiments, the dominant factor determining EUV emission from tin targets is not the opacity of the plasma, but the need to heat the plasma to temperatures where there is significant ionization in the range Sn^{7+} to Sn^{13+}. A threshold electron temperature greater than 20 eV is required to produce significant tin emission at 13.5 nm, while the emission (but not the escaping intensity) remains approximately constant at higher temperatures up to $\approx$ 60 eV (see Fujioka et al[13]).

We can use the scaling of optical depth for a laser-produced plasma EUV source shown in equation 17 to estimate the laser intensity for optimum EUV production with different laser wavelengths λ_L and laser pulse durations t_L. The fit to the experimental results shown in figure 5 indicates that the optimum EUV emission occurs with optical depth $\tau_0 \approx 1$ for a Gaussian profile. Re-arranging equation 17 gives the scaling for the laser intensity of optimum EUV emission for both Gaussian and Lorentzian profiles as

$$\frac{I_L[\mathrm{Wcm}^{-2}]}{10^{11}} \approx 4\left(\frac{\lambda_L[\mu\mathrm{m}]}{1.064}\right)^{4/5} (t_L[\mathrm{ns}])^{-9/5}. \quad (19)$$

As predicted by equation 19, a higher laser intensity for optimum EUV production has been observed using CO_2 lasers operating at wavelength 10.6 μm compared to Nd lasers operating at wavelength 1.06 μm[15]. As also predicted by equation 19, the laser intensity for optimum EUV production drops with increasing laser pulse duration (see simulations by Sunahara et al[16]).

Line emission at wavelengths greater than 13.5 nm can load unwanted energy onto EUV mirrors and ultimately reach the wafer surface in EUV lithography causing a degraded image contrast. Such high wavelength ‘out-of-band’ emission is expected to have a higher mass absorption coefficient in the plasma and following our model, the ‘out-of-band’ output from an EUV radiation source has a maximum at higher laser intensity than the 13.5 nm output. This argument is supported by measurements[17] showing conversion efficiencies of 123 - 400 nm light from an EUV source with a maximum at intensities 1 -2 $\times 10^{10}$ Wcm^{-2} for a 1.06 μm laser with a pulse duration of 10 ns. Assuming a mass absorption coefficient for the 123 - 400 nm radiation equal to the absorption coefficient at 13.5 nm implies a peak conversion efficiency at a lower laser intensity value of 6×10^9 Wcm^{-2}.

A potential successor to EUV lithography involves using shorter wavelengths near 6.7 nm, sometimes referred to as ‘beyond extreme ultra-violet lithography’ (BEUVL)[3,4]. Emission near 6.7 nm has been produced in laser-produced plasmas[18] with efficiency up to 0.8% using targets of Gd, Tb and Mo ionized in the range 12+ to 35+; that is with a charge approximately twice the charge required for tin emitting at 13.5 nm. Absorption coefficients for similar spectral lines scale approximately as $1/Z_i^2$, where Z_i is the ion charge (see Tallents[5]). Using this scaling, we can modify equations 17 and 18 by a simple multiplication of $1/Z_i^2 = 1/4$ to give, for example, a value of the average optical depth τ_{av}^* relevant to the production of 6.7 nm radiation. Modifying equation 17 we obtain

$$\tau_{av}^* \approx 0.27\left(\frac{I_L[\mathrm{Wcm}^{-2}]}{1.2\times 10^{12}}\right)^{5/9}\left(\frac{\lambda_L[\mu\mathrm{m}]}{1.064}\right)^{-4/9} t_L[\mathrm{ns}]. \quad (20)$$

Equation 20 illustrates that the escaping radiation emission near 6.7 nm has a line profile peak optical depth $\tau_0^* \approx 1$ at laser intensities $\approx$ 12 times greater than occurs for EUV radiation at 13.5 nm. We would expect a similar drop in the escaping radiation at 6.7 nm as shown in figure 5 except that the laser intensity scale is multiplied by 12. In good agreement with this derived scaling, experimental results[18] for the conversion efficiency of laser light to radiation 6.5 - 6.7 nm show a decrease with increasing laser intensity above $I_L \approx 10^{12}$ Wcm^{-2} .

IV. CONCLUSION

We have examined the escape of spectral line radiation from laser-produced plasma radiation sources with moderate opacity. A simple model of emission assuming a planar geometry, constant source function and varying optical depth has been employed to produce variations in emission relative to optically thin plasmas in agreement with previous experimental

measurements of both the angular variation of the emission of extreme ultra-violet (EUV) light at 13.5 nm and the effect of plasma opacity in reducing EUV emission from laser-produced plasmas at laser intensities above 10^{11} Wcm^{-2}. The simple model exhibits an experimentally observed drop in EUV radiation at laser intensities $> 10^{11}$ Wcm^{-2} and demonstrates that plasma optical depth increase with increasing laser intensity causes a fall in EUV production at laser intensities greater than an optimum value. Similar opacity arguments apply to a potential successor to EUV lithography, namely lithography at ≈ 6.7 nm, where it is shown that opacity effects reduce the escaping 6.7 nm radiation at laser intensities above 10^{12} Wcm^{-2}.

[1] N. N. Chapman, A. Barty, M. J. Bogan, and et al, "Femtosecond diffractive imaging with a soft-X-ray free-electron laser," Nature Phys. **2**, 839 – 843 (2006).

[2] E. Esarey, C. B. Schroeder, and W. P. Leemans, "Physics of laser-driven plasma-based electron accelerators," Rev. Mod. Phys. **81**, 1229 – 1285 (2009).

[3] G. J. Tallents, E. Wagenaars, and G. J. Pert, "Optical lithography: Lithography at EUV wavelengths," Nature photonics **4**, 809–811 (2010).

[4] G. O'Sullivan, L. Bowen, R. D'Arcy, and et al, "Spectroscopy of highly charged ions and its relevance to EUV and soft x-ray source development," J. Phys. B **48**, 144025 (2015).

[5] G. Tallents, *An introduction to the Atomic and Radiation Physics of Plasmas* (Cambridge University Press, 2018).

[6] F. E. Irons, "The escape factor in plasma spectroscopy I The escape factor defined and evaluated ," J. Quant. Spect. Rad. Trans. **22**, 1 – 20 (1979).

[7] S. J. Pestehe and G. J. Tallents, "Escape factors for laser-plasmas ," J. Quant. Spect. Rad. Trans. **72**, 853 – 878 (2001).

[8] D. Salzmann, "Escape factors in spherically symmetric plasmas ," J. Quant. Spect. Rad. Trans. **107**, 141–153 (2007).

[9] G. J. Phillips, J. S. Wark, F. M. Kerr, S. J. Rose, and R. W. Lee, "Escape factors in zero-dimensional radiation codes," High Energy Density Phys. **4**, 18–25 (2008).

[10] A. Ng, D. Pasini, P.Celliers, D. Parfeniuk, L. DaSilva, and J. Kwan, "Ablation scaling in steady-state ablation dominated by inverse bremsstrahlung absorption," Appl. Phys. Lett. **45**, 1046 – 1048 (1984).

[11] T. Ando, S. Fujioka, H. Nichimura, N. Ueda, and et al, "Optimum laser pulse duration for efficient extreme ultraviolet light generation from laser-produced tin plasmas," Appl. Phys. Lett. **89**, 151501 (2006).

[12] A. Z. Giovannini and R. S. Abhari, "Three-dimensional extreme ultraviolet emission from a droplet-based laser-produced plasma," J. Appl. Phys. **114**, 033303 (2013).

[13] S. Fujioka, H. Nishimura, K. Nishihara, A. Sasaki, and et al, "Opacity effect on extreme ultraviolet radiation from laser-produced tin plasmas," Phys. Rev. Lett. **95**, 235004 (2005).

[14] R. A. Burdt, S. Yuspeh, K. L. Sequoia, Y. Tao, M. S. Tillack, and F. Najmabadi, "Experimental scaling law for mass ablation rate from a Sn plasma generated by a 1064 nm laser," J. Appl. Phys. **106**, 033310 (2009).

[15] H. Tanaka, A. Matsumoto, K. Akinaga, A. Takahashi, and T. Okada, "Comparative study on emission characteristics of extreme ultraviolet radiation from CO_2 and Nd:YAG laser-produced tin plasmas," Appl. Phys. Lett. **87**, 041503 (2005).

[16] A. Sunahara, K. Nishihara, and A. Sasaki, "Optimization of extreme ultraviolet emission from laser-produced tin plasmas based on radiation hydrodynamics simulations," Japan Soc. Plasma Sci. Nucl. Fus. Res. **3**, 043 (2008).

[17] H. Parchamy, J. Szilagyi, M. Masnavi, and M. Richardson, "Ultraviolet out-of-band radiation studies in laser tin plasma sources," J. Appl. Phys. **122**, 173303 (2017).

[18] K. Yoshida, S. Fujioka, T. Higashiguchi, and et al, "Efficient extreme ultraviolet emission from one-dimensional spherical plasmas produced by multiple lasers," Appl. Phys. Express **7**, 086202 (2014).